

# Details Matter in Structure-based Drug Design

Bernd Kuhn<sup>§\*</sup>, Jens-Uwe Peters, Markus G. Rudolph, Peter Mohr, Martin Stahl, and Andreas Tosstorff

<sup>§</sup>SCS Senior Industrial Science Award 2022

**Abstract:** Successful structure-based drug design (SBDD) requires the optimization of interactions with the target protein and the minimization of ligand strain. Both factors are often modulated by small changes in the chemical structure which can lead to profound changes in the preferred conformation and interaction preferences of the ligand. We draw from examples of a Roche project targeting phosphodiesterase 10 to highlight that details matter in SBDD. Data mining in crystal structure databases can help to identify these sometimes subtle effects, but it is also a great resource to learn about molecular recognition in general and can be used as part of molecular design tools. We illustrate the use of the Cambridge Structural Database for identifying preferred structural motifs for intramolecular hydrogen bonding and of the Protein Data Bank for deriving propensities for protein–ligand interactions.

**Keywords:** Intramolecular hydrogen bond · Ligand strain · Molecular interactions · PDE10



**Bernd Kuhn** received his PhD at the Swiss Federal Institute of Technology at Lausanne (with T. Rizzo) and did postdoctoral research with P. Kollman at the University of California, San Francisco. After one year at Prospect Genomics he joined F. Hoffmann-La Roche in Basel in 2001 and he is currently a Distinguished Scientist in the CADD group. His scientific focus has been on new structure-based computational

methods and their application to drug design projects as well as on the study of molecular recognition of small molecules, which has led to a number of highly cited publications (h-index: 47). He has contributed to 10 compounds in clinical development and is co-author of ~140 patents. Among his awards are the Roche Patent Gold medal and the Roche Leo Sternbach Award for innovation in chemistry.

## 1. Introduction

Roche has pioneered structure- and property-based design for drug discovery<sup>[1]</sup> and I was fortunate enough to learn the key concepts from a number of excellent scientists when joining Roche in 2001. For example, mining of the Cambridge Structural Database (CSD)<sup>[2]</sup> and using this information for structure-based drug design (SBDD) has been instrumental for many successful compound designs with improved target binding or selectivity.<sup>[3]</sup> Capitalizing on small molecule crystal structure information during the design process is a highly rewarding and educational exercise as it sharpens the view for artefacts of computer-generated conformations or binding poses of ligands. Moreover, the CSD contains many examples which illustrate that details matter in SBDD, some of which will be highlighted in this article. Due to its value for design, our group, in collaboration with academic partners, has developed a number of software tools that make use of CSD information for scaffold hopping, assessment of ligand strain, and interaction searching.<sup>[4–8]</sup>

In a number of projects, a peculiar structure–activity or structure–property relationship (SAR/SPR) finding, which was diffi-

cult to rationalize with existing knowledge, triggered excursions into more general studies of molecular recognition or conformational effects. One example from a Roche legacy project will be discussed in the next section. In section 3, we present a case study of ligand strain, where small changes in chemical structure induced profound effects on the 3D geometry and on receptor binding. We close with a brief summary on the statistical significance of selected non-classical as well as strongly non-competitive protein–ligand interactions using a recently developed data mining approach.

## 2. From PDE10 Inhibitors to New Insights into Intramolecular Hydrogen Bonds

In the lead identification phase of a Roche project targeting phosphodiesterase 10A (PDE10) inhibitors as putative drugs against schizophrenia, we discovered a very strong gain in PDE10 inhibition by replacing a chlorine atom with *N,N*-dimethylcarboxamide (Fig. 1). X-ray crystal structures of PDE10 with the two ligands **1** and **2** revealed a strong hydrogen bond network of the benzimidazole amide core with the side chains of Tyr 693 and Gln 726. Interestingly, the additional amide substituent in **2** adopted a conformation involving a 7-membered intramolecular hydrogen bond (IMHB). Pyrazole and amide planes are twisted by 35° in the crystal structure. While the ~180-fold activity gain was surprising given the significant solvent exposure of the new substituent, the increase in experimental solubility and polarity was even less expected, as it runs contrary to the notion that burial of polar groups through formation of IMHB's should increase lipophilicity.

This lack of understanding of the effects of IMHBs on target inhibition and molecular properties triggered a systematic study involving small molecule crystal structure database searches and detailed characterization of model systems.<sup>[10]</sup> Statistical analyses of the CSD were used to derive propensities for IMHB formation of 5–8-membered rings. Planar 6-membered rings involving sp<sup>2</sup>-hybridized linker atoms showed the highest tendencies to form internal hydrogen bonds. Their high stability can be rationalized by enhanced  $\pi$ -electron delocalization in a strain-free geometry.

\*Correspondence: Dr. B. Kuhn, E-mail: bernd.kuhn@roche.com

Roche Pharma Research and Early Development, Innovation Center Basel, F. Hoffmann-La Roche Ltd., CH-4070 Basel, Switzerland

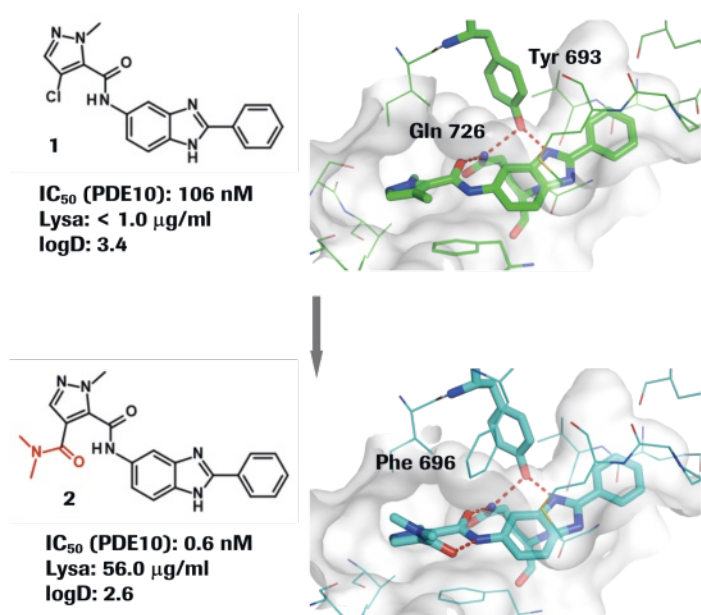


Fig. 1. Strong gain in PDE10 inhibitory effect and improvement in molecular properties by a simple molecular change (PDB codes: 5sji, 5sdw).<sup>[9]</sup> Human PDE10 IC<sub>50</sub> values were determined using a scintillation proximity binding assay.<sup>[9]</sup>

While these IMHB motifs offer many scaffold hopping opportunities for replacing a bicyclic aromatic ring, they typically do not lead to improved molecular properties.

Our studies revealed several interesting, yet poorly characterized 7-membered ring topologies that not only exhibit a high propensity to form IMHBs but, due to their non-planar shape, also come along with inherent favorable properties. Fig. 2a shows the first motif, which has one carbon sp<sup>3</sup> linker atom leading to a puckered ring geometry. Measurements of permeability, solubility, and lipophilicity were performed for a matched molecular pair containing a similar topology with one sp<sup>3</sup> linker atom and a methylated analogue which lacks the hydrogen bond donor necessary to form an IMHB (Fig. 2b). Formation of the IMHB in the 7-membered ring led to an increase in aqueous solubility, which is different from the behaviour of an analogous planar 6-membered ring system showing decreased solubility (Fig. 2c). Quantum-mechanical calculations suggested that for the 7-membered ring the hydrogen-bonded (apolar) conformation is strongly preferred in a low-dielectric environment, while in water the open (polar) conformation should also be significantly populated, positively affecting solubility. Typically, high water solubility combined with good membrane permeability are desirable features of a small molecule drug and therefore molecular structures with ‘chameleonic’ behavior,<sup>[11]</sup> which can adapt their shape and properties to the environment, are particularly relevant.

Another 7-membered IMHB motif with high propensity is present in our PDE10 inhibitor series and illustrated in Fig. 3. For this topology the preferred conformation depends subtly on the ring size of the connecting linker. An IMHB can be formed for 5-membered rings while the exit vectors in 6-membered rings are not compatible with a strain-free IMHB arrangement. The resulting conformations are vastly different and explain the drastic PDE10 inhibition loss when increasing the ring size of the connecting linker by just one atom (compounds **8** vs. **7**). This example nicely illustrates the importance of details in structure-based design.

Further SAR exploration around compounds **1** and **2** revealed that replacing the chlorine substituent with carboxamide or *N*-methylcarboxamide, resulting in primary and secondary amides, had only small effects on water solubility. These modifica-

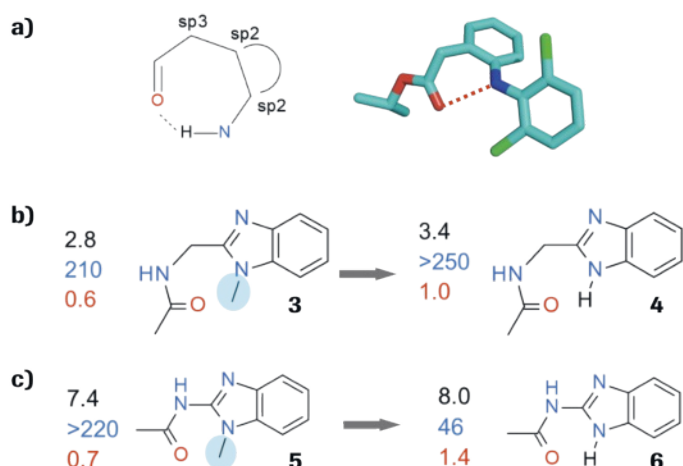


Fig. 2. a) 61% of all CSD entries with the depicted 7-membered ring topology show an IMHB geometry. Example CSD entry MISBEW is shown on the right. b) and c) PAMPA permeation constant Pe [ $10^{-6}$  cm/s] (black), LYSA water solubility [ $\mu$ g/ml] (blue), and octanol/water partition coefficient log D (red) for 7- and 6-membered IMHB model systems, respectively. The structures on the right are able to form an IMHB while the structures on the left cannot due to a missing hydrogen bond donor (blue circle).

tions led to the formation of an IMHB; however, as the geometry is planar, water solubility remained low. Formation of a non-planar conformation with a weak IMHB through tertiary amide substitution as in **2** was crucial to boost solubility. Clearly, this 3D conformational effect is not captured by simple lipophilicity models like clogP, which predicted an increase in lipophilicity due to the additional methyl groups. A similar trend could be observed for PDE10 inhibition with tertiary amides being exquisitely beneficial substituents. We attributed this to the non-planar arrangement allowing for a favorable edge-to-face  $\pi$ - $\pi$  interaction with neighboring Phe 696 (Fig. 1).

### 3. Know the Torsions of your Molecule

Ligand strain, *i.e.* the rise in internal energy of a ligand as a consequence of target binding, can be a major contribution to an observed potency loss. While equally important to the optimization of intermolecular interactions, it is typically much less dis-

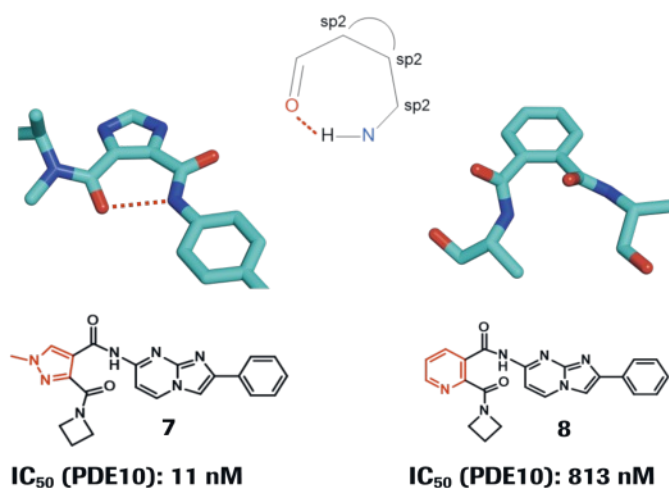


Fig. 3. 7-membered ring topology whose propensity to form an IMHB depends subtly on the ring system that is used in the linker. 5-membered rings are able to form IMHBs (left, CSD example: HEPHIU) while 6-membered rings do not (right, CSD example: LICKIS). This is reflected in large PDE10 inhibition differences for the two molecules **7** and **8**.

cussed. Analyzing how well torsion angles match the distribution in CSD statistics is an elegant way to assess ligand strain,<sup>[12]</sup> provided that the dihedral angle of interest is well sampled in small molecule crystal structures. The following example illustrates how the SAR in a series of PDE10 inhibitors could be understood and exploited for new designs taking both ligand strain and two key hydrogen bond interactions into account.

In the PDE10 selectivity pocket<sup>[13]</sup> next to Tyr 693 (Fig. 1), we probed different biaryl rings having in common an aromatic nitrogen lone pair as essential hydrogen bond acceptor for the interaction with the tyrosine hydroxyl group (Fig. 4). A good correlation between the calculated hydrogen bond acceptor strength of the ligand nitrogen,  $\text{clogK}_\beta$ , with  $\log \text{PDE10 IC}_{50}$  could be identified for compounds **1**, **9**, and **10**. Reduced acceptor strength and thus weaker hydrogen bond interaction with Tyr 693 resulted in weaker inhibition (blue circles in Fig. 4). This was very different for compounds **11** and **12** (red circles), where inhibitory activities were considerably weaker and stronger, respectively, than was predicted based on calculated hydrogen bond interaction strengths.

As the distinguishing feature in compounds **11** and **12** compared to the other ones is a ring nitrogen atom adjacent to the amide bond, we investigated whether potential ligand strain in the torsion connecting both fragments could contribute to the observed behavior. Fig. 5 shows that substantial differences exist between both compounds when mapping the torsional angle required for productive hydrogen bond interactions with Tyr 693 and Gln 726 on the CSD distribution. For compound **12** the key PDE10 hydrogen bonds can be formed in a strain-free ligand conformation, and we suggest this preorganization to be a substantial contributor to the very good inhibition constant of 7 nM. In contrast, compound **11** would need to bind in a highly strained conformation where nitrogen and carbonyl oxygen lone pairs strongly repel each other to make both hydrogen bonds with the protein. The very low population of this region in the CSD plot suggests substantial ligand strain, which is likely the reason for the ~17-fold higher  $\text{IC}_{50}$  value than what could be expected from the hydrogen bond interaction (**11** vs. **10**).

We speculated that due to the high ligand strain compound **11** might orient differently than the other analogues (Fig. 1), with the central amide carbonyl group pointing away from Gln 726 (Fig. 6). To probe this hypothesis we synthesized the secondary amide analogue **13**, which was originally not considered due to the comparably weak PDE10 inhibition of **11**. With this design it was possible to recover the hydrogen bond interaction with Gln 726, as confirmed by the crystal structure in Fig. 6, with a concomitant 5-fold improvement in the PDE10  $\text{IC}_{50}$ .

#### 4. Molecular Interactions for Drug Design

A recurring theme of our work has involved theoretical and experimental studies to better understand the nature of protein–ligand interactions relevant for structure-based drug design.<sup>[14–23]</sup> These focused on different types of non-classical interactions and were often performed in close collaboration with the research group of Prof. François Diederich (ETH Zurich), our long-term consultant and friend.<sup>[24]</sup>

More recently and based on a publication by Robin Taylor from the Cambridge Crystallographic Data Centre (CCDC), who introduced an elegant statistical treatment of interactions using CSD data,<sup>[25]</sup> we extended his ratio-of-frequencies ( $R_F$ ) approach to protein–ligand contact statistics derived from a curated version of the Protein Data Bank (PDB).<sup>[26]</sup> In the  $R_F$  framework the observed frequency of occurrence of a given protein–ligand contact type is compared against a statistical null model based on exposed surface areas.  $R_F$  values can be expressed as a function of interaction geometry and can be mapped onto the intermolecular contacts of a binding site of interest. Values greater than 1 indicate

competitive interactions that occur more often than expected by chance while the opposite is true for  $R_F < 1$ .

During the last decade a strikingly high number of unusual interaction types has been postulated to be favorable for protein–ligand binding. Using the  $R_F$  approach, we investigated the statistical significance of some of these interactions focusing on selected functional groups of relevance in medicinal chemistry<sup>[26]</sup> Fig. 7 shows some examples with high  $R_F$  values suggesting that these could be particularly attractive for structure-guided affinity optimization. These include  $\sigma$ -hole bonding of chlorine and

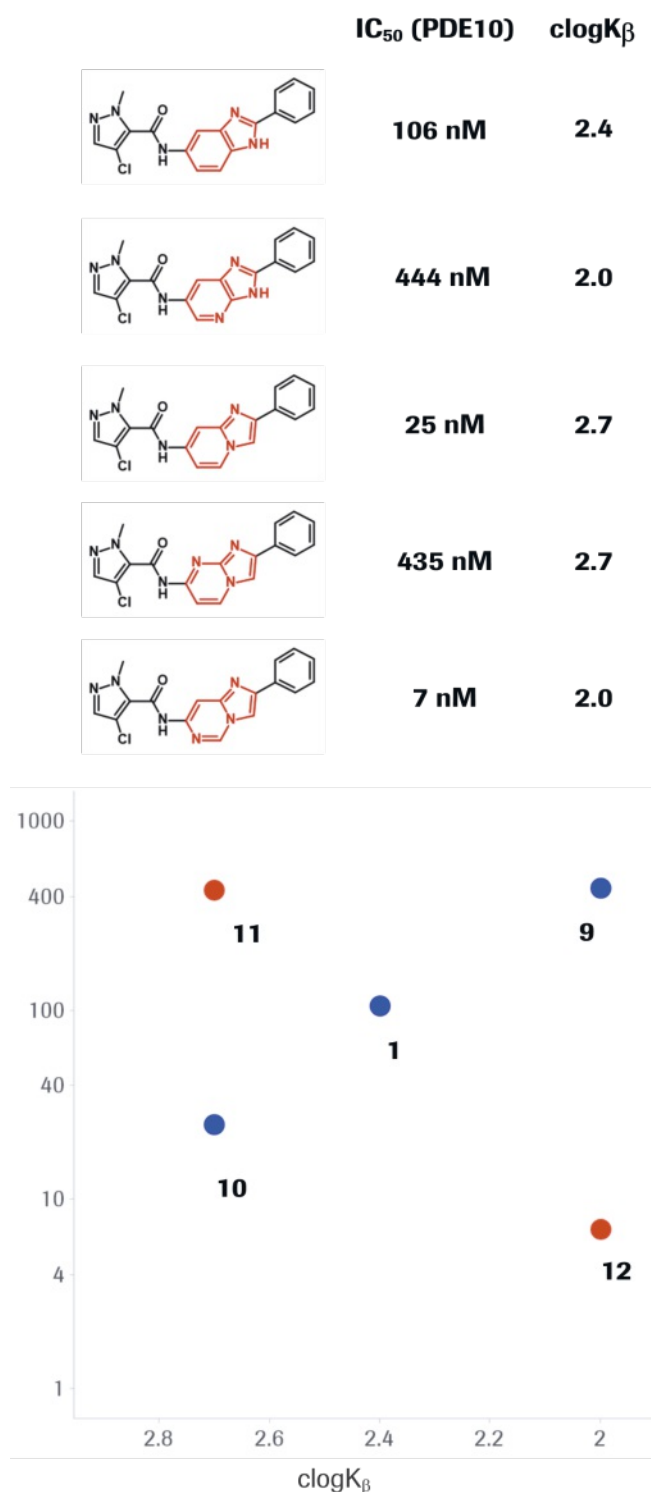


Fig. 4. SAR of PDE10 inhibitors featuring different aromatic heteroaryl rings for interaction with Tyr 693 (Fig. 1). Hydrogen bond acceptor strength  $\text{clogK}_\beta$  values were calculated with an internal tool based on electrostatic local minima along acceptor lone pair directions.

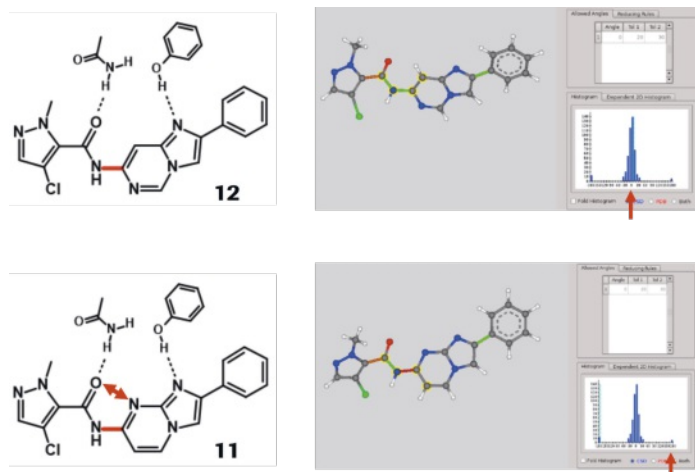


Fig. 5. Schematic illustration of desired PDE10 hydrogen bond interactions for compounds **11** and **12**, and comparison of their torsional angle between the ligand amide and biaryl groups in this PDE10 binding mode with the CSD distribution (red arrows on the right). The analysis was performed with the program Torsion Analyzer.<sup>[5,6]</sup>

heavier halogens with carbonyl oxygen atoms when aligned in a geometry as shown in Fig. 7 (Cl...O\_pi\_acc). Other examples include orthogonal multipolar fluorine or chlorine interactions with the carbon atom of amide groups (F/Cl...C\_pi\_carbonyl). We found several statistically significant competitive interactions of nitrile groups, for example with the guanidinium tail of arginine side chains (CN...N\_pi\_don\_pos), which have only been poorly studied so far. For other non-classical interactions such as weak hydrogen bonds of amide NH donors with fluorine atoms we saw no evidence that these occur more often than expected by chance. Our analysis suggests that the preferred alignment of fluorine is not in the amide plane where hydrogen bonding occurs but that a tilted geometry is preferred (Fig. 7, F...N\_pi\_don).

While many structure-based design tools focus on the visualization of protein–ligand interactions that are thought to be favorable, much less efforts have been devoted to highlighting potentially repulsive intermolecular contacts. This is usually limited to steric clash detection and sometimes to polar–apolar interaction pairs because of their expected desolvation cost upon binding. This is surprising as identification of a poor contact and resolving it with appropriate molecular design can lead to substantial affinity gains. In another  $R_F$  study we identified and discussed non-competitive interactions, *i.e.* with low  $R_F$  values, for different atom

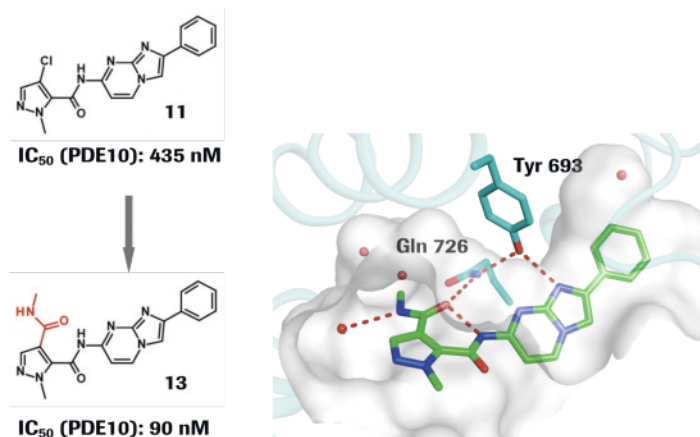


Fig. 6. Design to recover the interaction with Gln 726 and X-ray crystal structure of PDE10 with **13** (PDB code: 5sk1).<sup>[9]</sup>

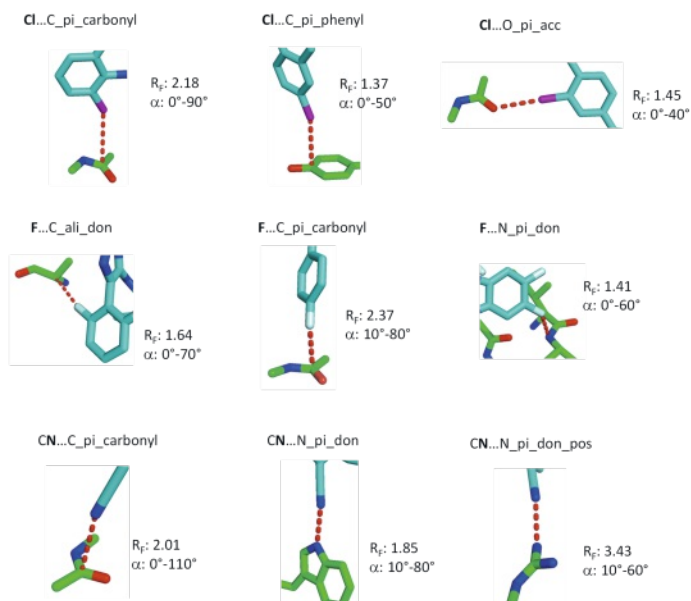


Fig. 7. Selected protein–ligand interaction types with high  $R_F$  values for chlorine (top), fluorine (middle), and cyano (bottom) groups. Definitions of protein atom types can be found in ref. [26].  $R_F$  values refer to the designated ranges of the interaction angle  $\alpha$ , which is defined by the ligand contact atom, its covalent neighbor atom, and the protein contact atom.

types.<sup>[27]</sup> Selected examples of such interactions, many of which can be rationalized by electrostatic repulsion or desolvation effects, are shown in Fig. 8. Obviously,  $R_F$  values are both atom type- and geometry-dependent and a non-competitive contact might be turned into a competitive one by changing one ligand atom or by interacting with the specific protein atom in a different geometry. The two faces of the interaction of chlorine atoms with carbonyl oxygen atoms (Cl...O\_pi\_acc) in Figs. 7 and 8 serve as an example.

Interactive 3D modeling sessions where project members come together to discuss new design ideas are an important component of successful SBDD.<sup>[24]</sup> To facilitate prioritization of the many proposals that are being evaluated in such meetings we have implemented the  $R_F$  analysis in a highly interactive and informative manner into the software MOE.<sup>[28]</sup> This is now routinely used in structure-enabled projects at Roche and also available to all interested scientists at their desktops.

## 5. Conclusions

The PDE10 project examples, the IMHB study, and the short excursion into protein–ligand interaction analysis illustrate some key guidelines that we think are important for efficient and successful structure-based drug design.

The vastly different propensities for IMHB formation for 5- vs. 6-membered aromatic linkers (Fig. 3) or the drastic changes in conformational preferences by shifting a ring nitrogen atom (Fig. 5) are testimony to the notion that details often matter in SBDD. We have found the CSD to be a very useful tool to become aware of these details and have profited from its content for the design of improved project compounds. Clearly, investigating changes in molecular interactions and conformations at a detailed level, and drawing the right design conclusions requires not only time and good software tools, but also a comprehensive knowledge of available project data and their uncertainties.

We have highlighted that ligand strain is an important component in molecular recognition and we think it should be given as much attention in the design process as the optimization of intermolecular contacts. Sometimes the easier way to improve target affinity is by reducing ligand strain rather than by opti-

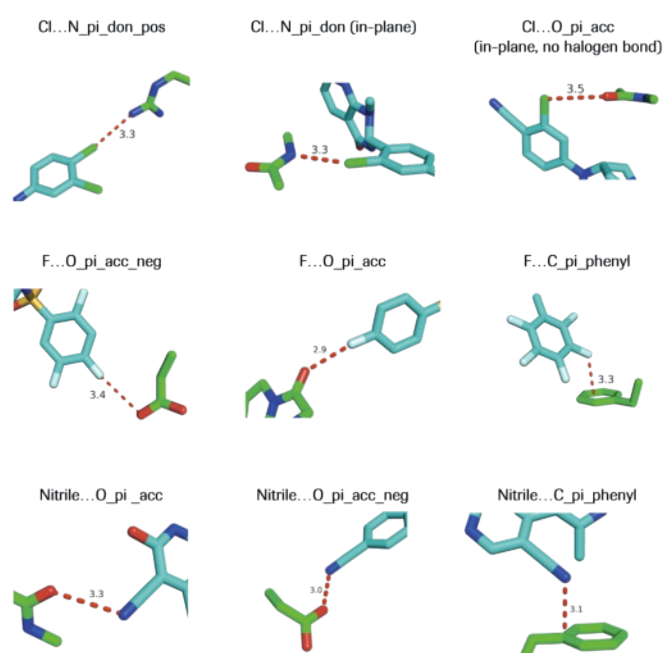


Fig. 8. Selected examples of non-competitive protein-ligand interactions with low  $R_F$  values. Definitions of protein atom types can be found in ref. [27]. The label next to the dashed line indicates the atom center distance in Angstrom.

mizing intermolecular interactions. Comparing the torsions in an experimental or modeled ligand structure with those found in the CSD or from high-accuracy calculations of torsional profiles can be means to achieve this.

Finally, since artefacts are easily introduced by a computational algorithm it is generally recommended to validate any model against relevant experimental data or to even incorporate such data if appropriate. We have built a tool that is based on statistical analyses of curated PDB data and are using it routinely to visualize potentially favorable and unfavorable interactions in a binding site. Apart from helping to educate the user on protein-ligand recognition the  $R_F$  interaction analysis tool has been successfully applied in the design of ligands with improved target binding.

### Acknowledgements

We would like to thank our colleagues at F. Hoffmann-La Roche for the many highly valuable contributions and discussions, in particular the members of the PDE10 project team. A special thanks goes to our collaboration partners Jason Cole and Robin Taylor from CCDC, Richard Bartelt from the Chemical Computing Group, and our colleagues Oliver Korb and Erik Gilberg for their contributions to the  $R_F$  work.

Received: April 24, 2023

- [1] K. Müller, *CHIMIA* **2014**, 68, 472, <https://doi.org/10.2533/chimia.2014.472>.
- [2] C. R. Groom, I. J. Bruno, M. P. Lightfoot, S. C. Ward, *Acta Cryst. B* **2016**, 72, 171, <https://doi.org/10.1107/S2052520616003954>.
- [3] B. Kuhn, W. Guba, J. Hert, D. Banner, C. Bissantz, S. Ceccarelli, W. Haap, M. Körner, A. Kuglstatler, C. Lerner, P. Mattei, W. Neidhart, E. Pinard, M. G. Rudolph, T. Schulz-Gasch, T. Woltering, M. Stahl, *J. Med. Chem.* **2016**, 59, 4087, <https://doi.org/10.1021/acs.jmedchem.5b01875>.
- [4] P. Maass, T. Schulz-Gasch, M. Stahl, M. Rarey, *J. Chem. Inf. Model.* **2007**, 47, 390, <https://doi.org/10.1021/ci060094h>.
- [5] C. Schärfer, T. Schulz-Gasch, H.-C. Ehrlich, W. Guba, M. Rarey, M. Stahl, *J. Med. Chem.* **2013**, 56, 2016, <https://doi.org/10.1021/jm3016816>.
- [6] W. Guba, A. Meyder, M. Rarey, J. Hert, *J. Chem. Inf. Model.* **2016**, 56, 1, <https://doi.org/10.1021/acs.jcim.5b00522>.
- [7] P. Penner, W. Guba, R. Schmidt, A. Meyder, M. Stahl, M. Rarey, *J. Chem. Inf. Model.* **2022**, 62, 1644, <https://doi.org/10.1021/acs.jcim.2c00043>.

- [8] O. Korb, B. Kuhn, J. Hert, N. Taylor, J. Cole, C. Groom, M. Stahl, *J. Med. Chem.* **2016**, 59, 4257, <https://doi.org/10.1021/acs.jmedchem.5b01756>.
- [9] A. Tosstorff, M. G. Rudolph, J. C. Cole, M. Reutlinger, C. Kramer, H. Schaffhauser, A. Nilly, A. Flohr, B. Kuhn, *J. Comput. Aided Mol. Des.* **2022**, 36, 753, <https://doi.org/10.1007/s10822-022-00478-x>.
- [10] B. Kuhn, P. Mohr, M. Stahl, *J. Med. Chem.* **2010**, 53, 2601, <https://doi.org/10.1021/jm100087s>.
- [11] G. Caron, J. Kihlberg, G. Ermondi, *Med. Res. Rev.* **2019**, 39, 1707, <https://doi.org/10.1002/med.21562>.
- [12] K. A. Brameld, B. Kuhn, D. C. Reuter, M. Stahl, *J. Chem. Inf. Model.* **2008**, 48, 1, <https://doi.org/10.1021/ci7002494>.
- [13] T. A. Chappie, C. J. Helal, X. Hou, *J. Med. Chem.* **2012**, 55, 7299, <https://doi.org/10.1021/jm3004976>.
- [14] C. Bissantz, B. Kuhn, M. Stahl, *J. Med. Chem.* **2010**, 53, 5061, <https://doi.org/10.1021/jm100112j>.
- [15] L. A. Hardegger, B. Kuhn, B. Spinnler, L. Anselm, R. Ecabert, M. Stihle, B. Gsell, R. Thoma, J. Diez, J. Benz, J.-M. Plancher, G. Hartmann, D. W. Banner, W. Haap, F. Diederich, *Angew. Chem. Int. Ed.* **2011**, 50, 314, <https://doi.org/10.1002/anie.201006781>.
- [16] L. A. Hardegger, B. Kuhn, B. Spinnler, L. Anselm, R. Ecabert, M. Stihle, B. Gsell, R. Thoma, J. Diez, J. Benz, J.-M. Plancher, G. Hartmann, Y. Isshiki, K. Morikami, N. Shimma, W. Haap, D. W. Banner, F. Diederich, *ChemMedChem* **2011**, 6, 2048, <https://doi.org/10.1002/cmcd.201100353>.
- [17] B. Kuhn, J. E. Fuchs, M. Reutlinger, M. Stahl, N. R. Taylor, *J. Chem. Inf. Model.* **2011**, 51, 3180, <https://doi.org/10.1021/ci200319e>.
- [18] M. Harder, B. Kuhn, F. Diederich, *ChemMedChem* **2013**, 8, 397, <https://doi.org/10.1002/cmcd.201200512>.
- [19] M. Harder, M. A. Carnero Corrales, N. Trapp, B. Kuhn, F. Diederich, *Chem. Eur. J.* **2015**, 21, 8455, <https://doi.org/10.1002/chem.201500462>.
- [20] B. S. Lauber, L. A. Hardegger, A. K. Asraful, B. A. Lund, O. Dumele, M. Harder, B. Kuhn, R. A. Engh, F. Diederich, *Chem. Eur. J.* **2016**, 22, 211, <https://doi.org/10.1002/chem.201503552>.
- [21] M. Giroud, M. Harder, B. Kuhn, W. Haap, N. Trapp, W. B. Schweizer, T. Schirmeister, F. Diederich, *ChemMedChem* **2016**, 11, 1042, <https://doi.org/10.1002/cmcd.201600132>.
- [22] M. Giroud, J. Ivkovic, M. Martignoni, M. Fleuti, N. Trapp, W. Haap, A. Kuglstatler, J. Benz, B. Kuhn, T. Schirmeister, F. Diederich, *ChemMedChem* **2017**, 12, 257, <https://doi.org/10.1002/cmcd.201600563>.
- [23] L.-J. Riwar, N. Trapp, B. Kuhn, *Angew. Chem. Int. Ed.* **2017**, 56, 11252, <https://doi.org/10.1002/anie.201703744>.
- [24] B. Kuhn, W. Haap, U. Obst-Sander, C. Kramer, M. Stahl, *ChemMedChem* **2021**, 16, 2760, <https://doi.org/10.1002/cmcd.202100351>.
- [25] R. Taylor, *CrystEngComm* **2014**, 16, 6852, <https://doi.org/10.1039/C4CE00452C>.
- [26] B. Kuhn, E. Gilberg, R. Taylor, J. Cole, O. Korb, *J. Med. Chem.* **2019**, 62, 10441, <https://doi.org/10.1021/acs.jmedchem.9b01545>.
- [27] A. Tosstorff, J. C. Cole, R. Taylor, S. F. Harris, B. Kuhn, *J. Chem. Inf. Model.* **2020**, 60, 6595, <https://doi.org/10.1021/acs.jcim.0c00858>.
- [28] A. Tosstorff, J. C. Cole, R. Bartelt, B. Kuhn, *ChemMedChem* **2021**, 16, 3428, <https://doi.org/10.1002/cmcd.202100387>.

### License and Terms



This is an Open Access article under the terms of the Creative Commons Attribution License CC BY 4.0. The material may not be used for commercial purposes.

The license is subject to the CHIMIA terms and conditions: (<https://chimia.ch/chimia/about>).

The definitive version of this article is the electronic one that can be found at <https://doi.org/10.2533/chimia.2023.489>